Fish and Shellfish Immunology 86 (2019) 46–52

Contents lists available at ScienceDirect

Fish and Shellfish Immunology

journal homepage: www.elsevier.com/locate/fsi

Full length article

Transcriptomic profiles of striped snakehead cells (SSN-1) infected with snakehead vesiculovirus (SHVV) identifying IFI35 as a positive factor for SHVV replication

Xiaodan Liu[a], Zhendong Qin[b], Sarath Babu V[b], Lijuan Zhao[b], Jun Li[c,d], Xiaojun Zhang[a,*], Li Lin[b,d,**]

[a] College of Animal Science and Technology, Yangzhou University, Yangzhou, 225009, China
[b] Guangdong Provincial Water Environment and Aquatic Products Security Engineering Technology Research Center, Guangzhou Key Laboratory of Aquatic Animal Diseases and Waterfowl Breeding, Guangdong Provincial Key Laboratory of Waterfowl Healthy Breeding, College of Animal Sciences and Technology, Zhongkai University of Agriculture and Engineering, Guangzhou, Guangdong, 510225, China
[c] School of Biological Sciences, Lake Superior State University, Sault Ste. Marie, MI, 49783, USA
[d] Laboratory for Marine Fisheries Science and Food Production Processes, Qingdao National Laboratory for Marine Science and Technology, Qingdao, 266071, China

ARTICLE INFO

Keywords:
Transcriptomic sequence
SSN-1
SHVV
Differentially expressed genes
IFI35

ABSTRACT

Snakehead vesiculovirus (SHVV) has caused great economic loss in snakehead fish culture in China. However, there is no effective strategy to prevent the epidemic of the virus. Understanding the host factors in response to virus infection is the basis for the prevention of viral disease. In this study, the transcriptomic profiles of SHVV-infected and mock-infected SSN-1 cells (derived from striped snakehead, Channa striatus) at 3 and 24 h (h) post of infection (poi) were obtained using high-throughput sequencing technique. A total of 93,372 unigenes were obtained. The differently expressed genes (DEGs) of SSN-1 cells upon SHVV infection were thereby identified, including 3668 and 3536 DEGs at 3 and 24 h poi, respectively. These DEGs were involved in many pathways of viral pathogenesis, including retinoic acid-inducible gene I (RIG-I) like receptors pathway, Toll-like receptor signaling pathway, NF-kappa B signaling pathway, PI3K-Akt signaling pathway and MAPK signaling pathway. Therefore, several immune-related DEGs were randomly selected and confirmed by quantitative real-time PCR (qRT-PCR). In addition, the effects of the interferon inducible protein 35 (IFI35) on SHVV replication were further investigated. Over-expression or inhibition of IFI35 significantly promoted or reduced SHVV replication at the level of viral gene expression, which indicated that IFI35 might be a positive factor for SHVV replication in SSN-1 cells. Our findings presented some valuable information, which will benefit for future study on SHVV-host interactions.

1. Introduction

Rhabdoviruses have a particularly broad host range, including plants, crustacean, insects, fish, and mammals [1]. To date, more than ten rhabdoviruses were identified in fish species, including Pike fry rhabdovirus (PRV) [2], Hirame rhabdovirus (HIRRV) [3], Infectious hematopoietic necrosis virus (IHNV) [4], Snakehead rhabdovirus (SHRV) [5], Viral hemorrhagic septicemia virus (VHSV) [6], Spring viraemia of carp virus (SVCV) [7], Chinese sucker rhabdovirus (CSRV) [8], *Scophthalmus maximus* rhabdovirus (SMRV) [9], *Siniperca chuatsi* rhabdovirus (SCRV) [10,11], *Monopterus albus* rhabdovirus (MoARV) [12], hybrid snakehead rhabdovirus [13]. In 2014, a new fish rhabdovirus called snakehead vesiculovirus (SHVV) was isolated from diseased hybrid snakehead fish cultured in Guangdong province, China [14]. SHVV has caused great mass mortality in snakehead fish culture in China these years. However, the molecular networks of host cells after SHVV infection were elusive.

High-throughput sequencing technology has exerted profound impact on the biological science research and provided valuable information for understanding of pathogen-host interactions [15–17]. In this report, we analyzed the transcriptomic profiles of striped snakehead cells (SSN-1) with or without SHVV infection by high-throughput

* Corresponding author.
** Corresponding author. Laboratory for Marine Fisheries Science and Food Production Processes, Qingdao National Laboratory for Marine Science and Technology, Qingdao, 266071, China.
E-mail addresses: zxj9307@163.com (X. Zhang), linli@zhku.edu.cn (L. Lin).

https://doi.org/10.1016/j.fsi.2018.11.031
Received 9 September 2018; Received in revised form 9 November 2018; Accepted 13 November 2018
Available online 14 November 2018

sequencing technique. From transcriptomic sequencing data, a large number of unigenes were annotated, and differently expressed genes (DEGs) were identified. The DEGs were involved in many functional categories and pathways of viral pathogenesis. Particularly, we estimated the effects of an interferon-stimulated gene IFI35 on SHVV replication, and found that it was a positive factor for SHVV replication. These results offered insight into the complexity of the virus-host interactions, and will shed a new light on the mechanisms of SHVV pathogenesis.

2. Material and methods

2.1. Cells and virus

SSN-1 cell was originated from the fish striped snakehead fry. It was kindly provided by Dr. Hong Liu from Shenzhen Animal & Plant Inspection and Quarantine Technology Center. SSN-1 cells were maintained in minimal essential medium (Invitrogen) supplemented with 10% FBS (Gibco) at 28 °C with 5% CO2. SHVV was isolated and stored in our lab [14].

2.2. Library construction and illumina sequencing

The SSN-1 cells were infected with 0.1 multiplicity of infection (MOI) of SHVV. At 3 and 24 h poi, SHVV-infected and mock-infected cells were collected in 1 ml TRIzol reagent (Invitrogen, USA) for the total RNA extraction according to the manufacturer's instructions. The mRNA was extracted from 5 μg of total RNA of the four samples: SSN-1 cell (3 h), SSN-1 cell infected with SHVV (3 h), SSN-1 cell (24 h), SSN-1 cell infected with SHVV (24 h) after DNase treatment and purification by oligo (dT) magnetic beads. RNAs were chemically fragmented into short fragments (about 200 bp) by using the RNA fragmentation buffer. The first strand cDNA was synthesized with random hexamer primer. RNase H, dNTP, and DNA polymerase I. The double-stranded cDNAs were purified with QiaQuick PCR extraction kit (Qiagen). The end of purified double-stranded cDNA were prepaired and added with polyA tails and adapter connector for sequencing. After the quality inspection of the cDNA library by Agilent 2100 Bioanalyzer, Illumina HiSeqTM 2000 was applied. Transcript sequence was jointed with Trinity (version:trinityrnaseq_r20131110) according to paired-end jointed method. Unigenes were finally obtained after Clustering to redundancy using TGICL software. Unigene expression abundance was calculated by bowtie2 (http://bowtie-bio.sourceforge.net/bowtie2/index.shtml) and eXpress (http://bio.math.berkeley.edu/eXpress).

2.3. Functional annotation and GO/KEGG enrichment analysis of transcriptomic sequencing

Data filtering including removing adaptors and low quality reads from raw reads was analyzed with NGS QC TOOLKIT v2.3.3 [18] (http://59.163.192.90:8080/ngsqctoolkit/). Data contamination was detected according to database alignment. The unigenes were annotated with databases of NCBI NR, SWISSPROT, and KOG. The genetic similarity was based on BLAST arithmetic [19]. The results of BlastX annotation were uploaded on Blast 2 Go to generate Gene Ontology annotations and mapped to the categories of GO database ((geneontology.org/page/download-annotations) and the Kyto Encyclopedia Genes and Genomes (KEGG) [20]. All the differential expressed unigenes were mapped to KEGG database ($p < 0.05$). Signaling pathways that GO and DEGs items participated in were mapped back to the GO and KEGG databases. The results were compared with the database and annotations of every gene for subsequent experimental analysis.

Table 1
Primers used for the detection of DEGs and SHVV genes by qRT-PCR.

Gene name	Forward primer (5′-3′)	Backward primer (5′-3′)
RIG-I	CATATTCCAGCGCTGTCTCA	ATCTTCAACACCGGCAAATC
IFI35	TCACTCCCTTTCTCAACGGC	CGGTTTGGACGTGTCCTCTT
TRAF3	CGTAGTGATGCGTGGTGAGT	ATGTAGGTGCCGTTCTCCAG
IRF3	CGTTGGGGAGACAGTCGTAT	ATGGTTTGTTCTTGGGGTCA
MAVS	TGTGAGGCAGGGCAAGTAAG	CTCGATCGGAAGTGCTGTGT
IRF7	GTACAAATATGCTAGAGGGCT	GGTTCTCACCTCTGTGAAG
IL12	TCCAGCACACTCACGTTGTT	CAACGACTGGCTGACTCTGT
SHVV-N	CCGCATCGGAAATCAAGCAG	GTTGACCGCTTGCCCAATTT
SHVV-P	ACAGCTATCCTCAAGCCGTG	ACAGCACCATTTGCTGAACC
Beta-actin	CACTGTGCCCATCTACGAG	CCATCTCCTGCTCGAAGTC

(RIG-I: Retinoic acid-inducible protein I; IFI35: Interferon inducible protein 35; TRAF3: TNF receptor associated factor 3; IRF3: Interferon regulatory factor 3; MAVS: Mitochondrial antiviral signaling; IRF7: Interferon regulatory factor 7; IL12: Interleukin 12; SHVV-N: the N gene of SHVV; SHVV-P: the P gene of SHVV.).

2.4. Analysis of gene expression by quantitative real-time PCR (qRT-PCR)

The reverse transcription reaction is in a total volume of 10 μl, consisted of 0.5 μg RNA, 2 μl of PrimerScript Buffer, 0.5 μl of oligo dT, 0.5 μl of random 6mers and 0.5 μl of PrimerScript RT Enzyme Mix I (TaKaRa, Japan). Reactions were performed at 37 °C for 15 min, followed by heat inactivation of RT for 5 s at 85 °C. The 10 μl RT reaction mix was then diluted 10 times in nuclease-free water and held at −20 °C. Real-time PCR was performed with 10 μl PCR reaction mixture including 1 μl of cDNA, 5 μl of 2 × LightCycler® 480 SYBR Green I Master (Roche, Swiss), 0.2 μl of forward primer, 0.2 μl of reverse primer (Table 1) and 3.6 μl of nuclease-free water. Reactions were incubated at 95 °C for 10 min, followed by 40 cycles of 95 °C for 10 s, 60 °C for 30 s. Each sample was run in triplicate for analysis. At the end of the PCR cycles, melting curve analysis was performed to validate the specific generation of the expected PCR product. The relative expression ratio of the target genes versus beta actin gene was calculated using 2-ΔΔCT method, and all data were given in terms of relative mRNA expression [21].

2.5. Investigation of IFI35 in SHVV infected SSN-1 cells

The plasmid pEYFP-IFI35 was generated by cloning the cDNA encoding the full-length open reading frame of IFI35 into pEYFP-N1 using primers of 5′-CGGGAATTCATGTCTTCAGATGAGGATTTC-3′, 5‘-ATGG ATCCCGCTCCGGT

TTGGACGTGTCCTC-3‘. For depletion of endogenous IFI35, small interfering RNA (siRNA): 5′-GCACGGCGUUUAUCACCUUtt-3′ was synthesized (GenePharma, China). A nontargeting siRNA: 5′-UUCUCCGA ACGUGUCACGUtt-3′ was used as negative control. All siRNA were used at a final concentration of 100 nM. The siRNA transfection was performed using Lipofectamine® 2000 Transfection Reagent (Invitrogen). At 24 h post transfection of the overexpressed plasmid and 36 h post transfection of the siRNA, cells were infected with SHVV (MOI = 0.1) for 24 h, and then the mRNA level of N and P gene of SHVV were estimated from the cells.

3. Results

3.1. DE NOVO assembly and functional annotation

The cDNA fragments from SHVV-infected or mock-infected SSN-1 cells at 3 and 24 h poi were purified by agarose gel electrophoresis and enriched by PCR amplification. High-quality cDNA libraries were generated and sequenced using Illumina HiSeq™ 2000 system. After removing adaptors and low quality reads, a total of 62,744,902, 68,899,840, 63,759,364, and 56,511,204 clean reads were obtained

Table 2
Summary of de novo assembly of transcriptomic sequencing.

Sample	Raw reads	Clean reads	Valid ratio
SSN-1 cell (3 h)	63155040	62744902	98.87%
SSN-1 cell infected with SHVV (3 h)	69303404	68899840	98.94%
SSN-1 cell (24 h)	64175020	63759364	98.88%
SSN-1 cell infected with SHVV (24 h)	56864566	56511204	98.92%

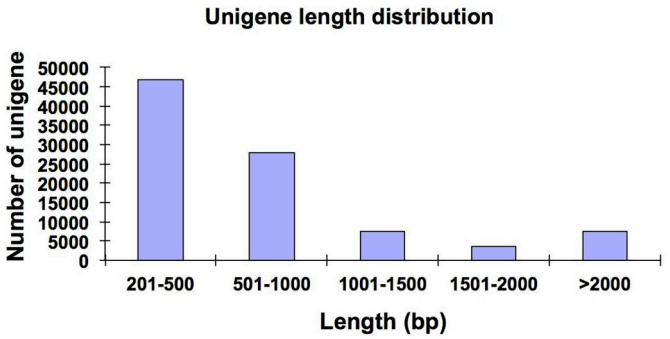

Fig. 1. Length distribution of unigenes from transcriptomic sequencing data. The x-axis indicates unigene size and the y-axis indicates the number of unigenes with different lengths.

Table 3
Annotation of unigenes of transcriptomic sequencing.

Database	Number of annotated unigenes	Percentage of annotated unigenes
NR	18,870	2021%
Swiss-Prot	15,716	1683%
KOG	12,947	1387%
GO	13,524	14.48%
KEGG	6404	6.86%

respectively from the four samples: SSN-1 cell (3 h), SSN-1 cell infected with SHVV (3 h), SSN-1 cell (24 h), and SSN-1 cell infected with SHVV (24 h) (Table 2). After de novo assembly, 93,372 unigenes were obtained by paired-end method of Trinity [22] and TGICL [23]. The mean contig length was 829 bp, ranging from 201 bp to 21,558 bp. The unigene size distribution was shown in Fig. 1. The most abundant unigenes were clustered in a group with 301–400 bp in length.

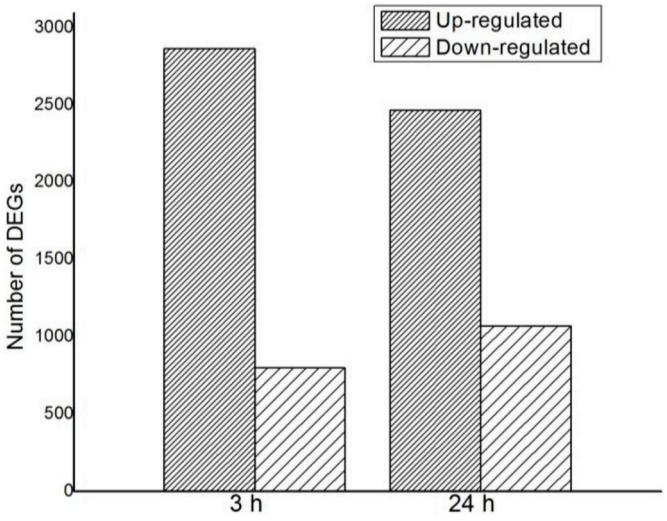

Fig. 3. The number of DEGs between SHVV-infected and mock-infected SSN-1 cells. The numbers of DEGs at 3 h and 24 h represented the differentially expressed genes at the two time points when the unigenes of SHVV-infected SSN-1 cells were compared to that of mock-infected SSN-1 cells.

The unigenes were blasted against several databases including the NCBI non-redundant (NR), SWISS-PROT, KEGG, GO and KOG. The numbers of annotated unigenes were varied (Table 3): NR (18,870, 20.21%), Swiss-Prot (15,716, 16.83%), KOG (12,947, 13.87%), GO (13,524, 14.48%), and KEGG (6,404, 6.86%).

In total, 12,947 unigenes were assigned to KOG classification and divided into 25 specific categories. The most abundant category was “Signal transduction mechanisms”, followed by “General function prediction only” and “Posttranslational modification, protein turnover, chaperones” (Fig. 2).

3.2. Analysis of differentially expressed genes (DEGs)

To identify the DEGs in SSN-1 cells potentially involved in SHVV infection, a statistical analysis of unigenes was conducted using fold change > 1.5 and p-value < 0.05 as standards. Compared to the mock-infected group, a total of 3668 and 3536 DEGs were identified at 3 h (or 24 h) poi in SHVV-infected group, including 2867 (or 2468) up-regulated genes and 801 (or 1068) down-regulated genes at 3 h (or

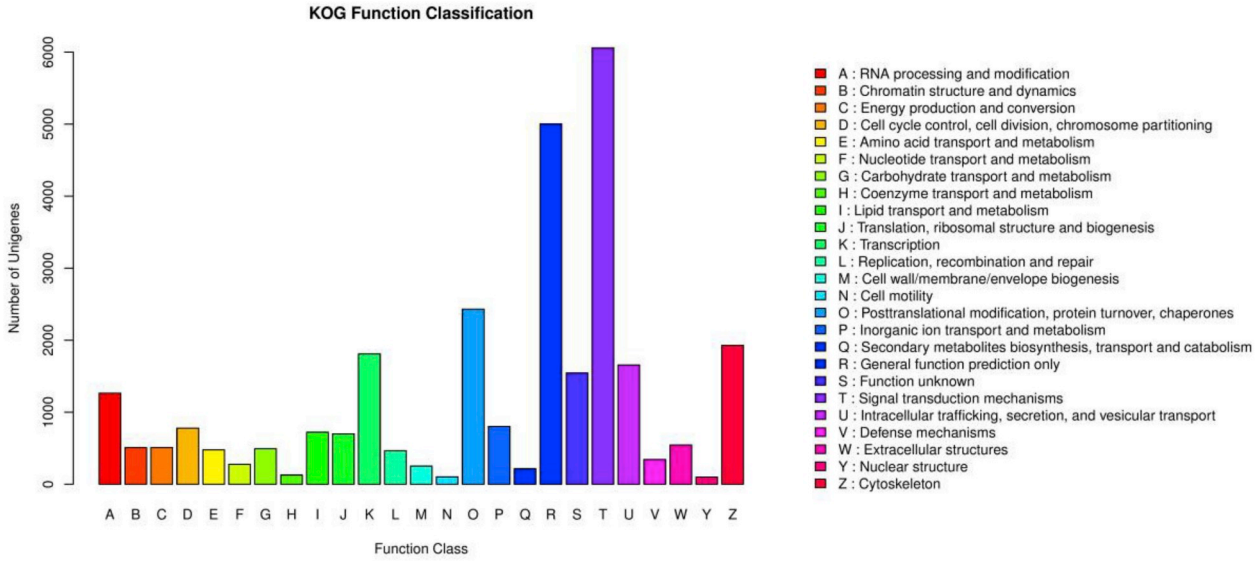

Fig. 2. KOG functional categories of the unigenes. The x-axis indicates 25 groups of KOG categories. The y-axis indicates the percentage of the number of unigenes.

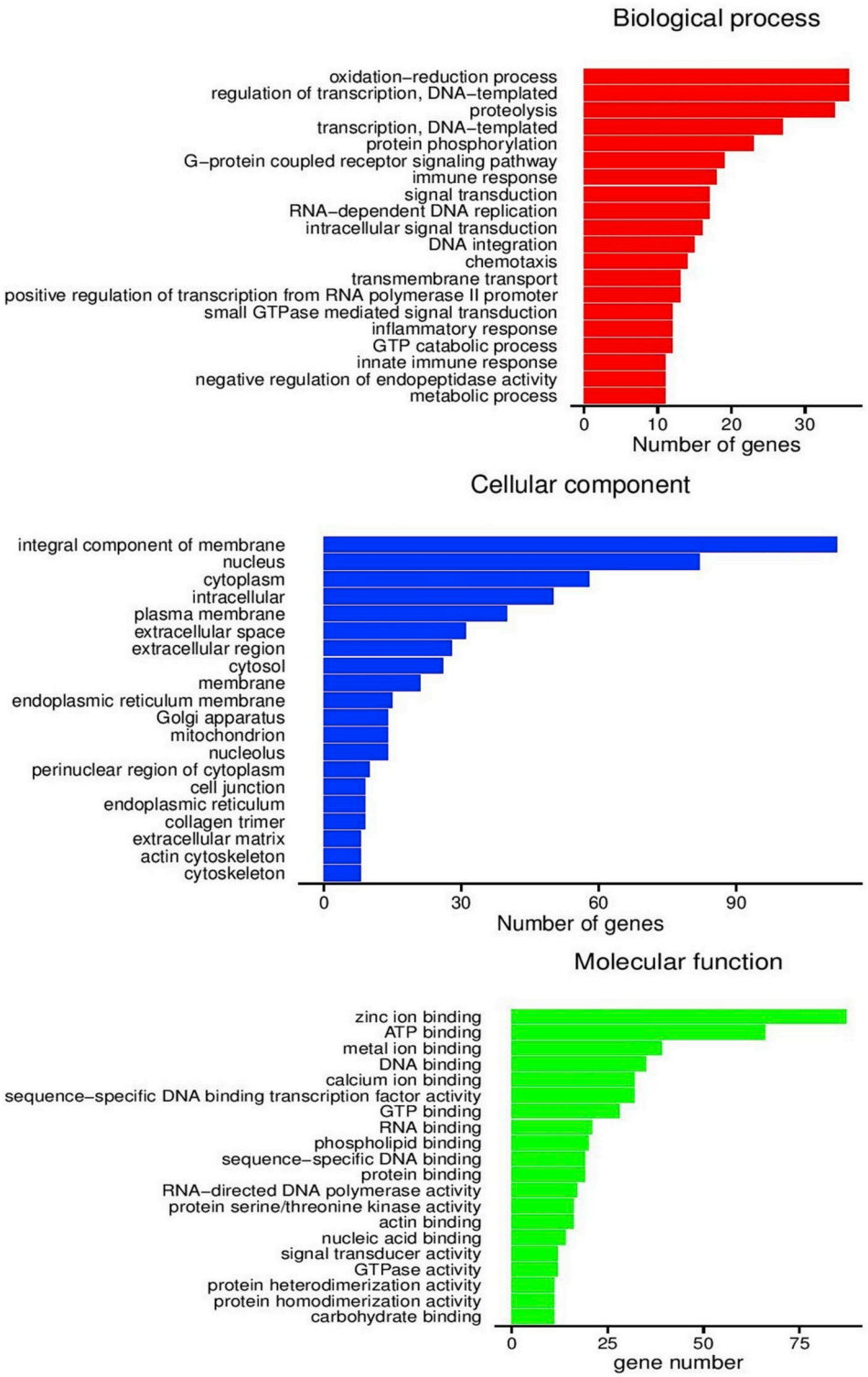

Fig. 4. GO enrichment analysis of the DEGs between SHVV-infected and mock-infected SSN-1 cells at 24 h. The x-axis is the number of unigenes, while the y-axis is gene functional classification including three major parts: biological process, cellular component, and molecular function.

24 h) poi (Fig. 3).

3.3. GO and KEGG analysis of the DEGs

To understand the biological processes in which the DEGs might be involved, the GO enrichment analysis was performed for the DEGs. GO analysis showed that a total of 1714 or 1742 DEGs were respectively annotated at 3 or 24 h poi. The DEGs at 3 and 24 h poi were classified into three subclasses (Fig. S1 and Fig. 4): biological processes, cellular components, and molecular functions. In the biological process subclass, the most abundant category at 3 and 24 h poi were “regulation of transcription, DNA-templated process” and “proteolysis process”. In the cellular component subclass, the top three categories at both 3 and 24 h poi were “integral component of membrane”, “nucleus”, and “cytoplasm”. In the molecular function subclass, the most abundant category at 3 and 24 h poi were “zinc ion binding” (Fig. S1 and Fig. 4). KEGG

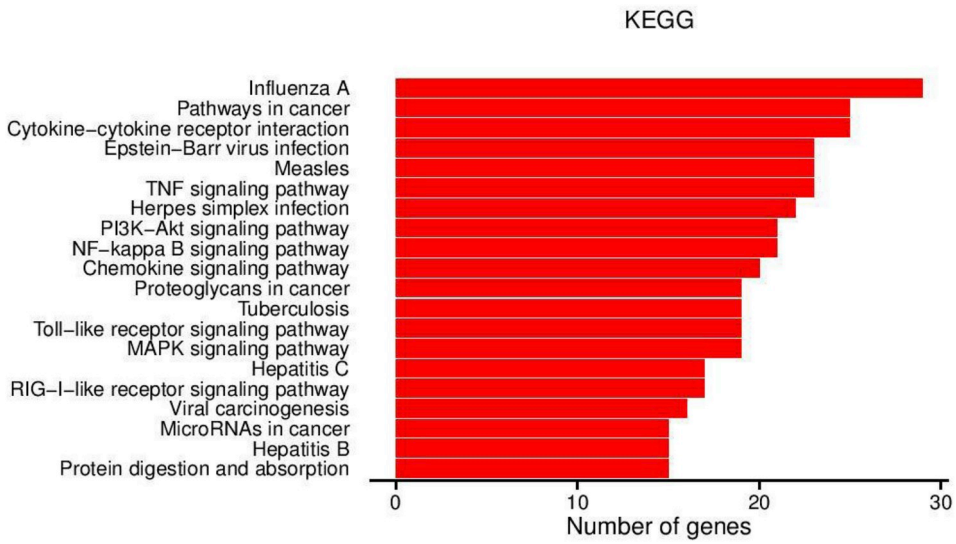

Fig. 5. KEGG pathway enrichment analysis of the DEGs between SHVV-infected and mock-infected SSN-1 cells at 24 h. The x-axis is gene number, while the y-axis is KEGG pathway classification.

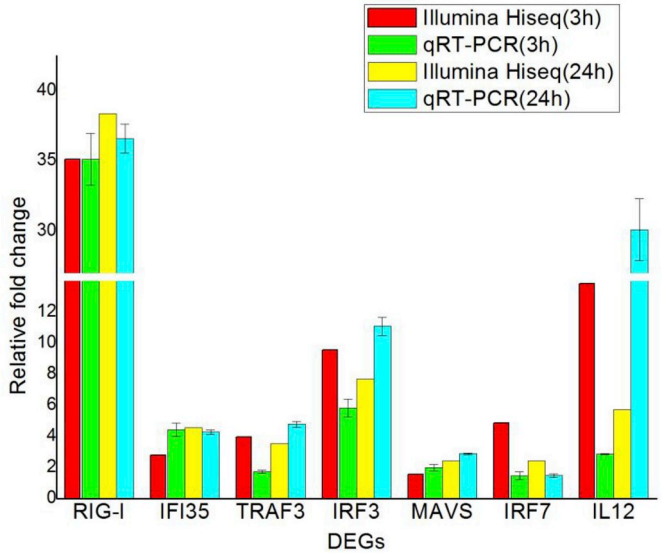

Fig. 6. Comparison of the expressions of seven DEGs determined by Illumina HiSeq™ 2000 sequencing and qRT-PCR. The x-axis displays seven genes and y-axis is the relative fold change. (Retinoic acid-inducible protein I (RIG-I), Interferon inducible protein 35 (IFI35), TNF receptor associated factor 3 (TRAF3), Interferon regulatory factor 3 (IRF3), Mitochondrial antiviral signaling (MAVS), IFN-regulatory factory 7 (IRF7), Interleukin 12 (IL12)).

analysis revealed that all the DEGs were assigned to 222 or 260 KEGG pathways at 3 or 24 h poi (Fig. S2 and Fig. 5). These DEGs were enriched in serials of immune-related pathways, including RIG-I like receptors pathway, Toll-like receptor signaling pathway, NF-kappa B signaling pathway, PI3K-Akt signaling pathway, and MAPK signaling pathway.

3.4. Verification of the DEGs by qRT-PCR

To verify the transcriptomic data, seven DEGs were randomly selected to validate the results by qRT-PCR. As shown in the Fig. 6, the qRT-PCR results exhibited similar expression tendency as the high-throughput sequencing data. The qRT-PCR analysis confirmed the expressions of DEGs detected by the high-throughput sequencing analysis.

3.5. IFI35 positively regulated SHVV replication in SSN-1 cells

A large number of DEGs were identified. We put emphasis upon the anti-viral immune system. From the transcriptome results, the IFN-I system was triggered by SHVV infection, which will lead to the generation of serials of interferon-stimulated genes (ISGs). One of the ISGs, the interferon inducible protein 35 (IFI35) was significantly up regulated during SHVV infection.

To investigate the role of IFI35 in SHVV infection, we generated a plasmid pEYFP-IFI35 and synthesized siRNA targeting the open reading frame of IFI35 to over-express or inhibit IFI35. Increased expression of IFI35 was observed after pEYFP-IFI35 was transfected into SSN-1 cells (Fig. 7A), while decreased expression of IFI35 was observed when siRNA of IFI35 was transfected (Fig. 7B). We took N and P gene expression as the measurement of virus replication. SHVV growth was enhanced significantly after overexpression of IFI35 (Fig. 7). A 5-fold reduction in SHVV N gene and P gene mRNA level were also observed in SSN-1 cells after siRNA of IFI35 transfection compared to the levels in negative siRNA treated control cells (Fig. 7). Over expression of IFI35 in SSN-1 cells decreased the mRNA level of key genes (RIG-I , MAV-S , TRAF3 , IRF3 , IRF7) in RIG-I pathway (Fig. 8). Similarly, inhibition of IFI35 expression reduced the mRNA level of genes in RIG-I pathway. These data suggested that IFI35 as a positive factor for SHVV replication according to RIG-I pathway.

4. Discussion

SHVV is a newly isolated fish rhabdovirus from diseased hybrid snakehead and has caused mass mortality to cultured snakehead fish in recent years in China, resulting in enormous economic losses in snakehead fish culture. Snakehead fish is one of the most economic and important fish species in China. Different from other economically important cultured fish species in China, such as *Ctenopharyngodon idella*, *Ictalurus punctatus*, *Larimichthys crocea*, the transcript sequence or genome information is available for functional genomic studies [24–26]. But for snakehead fish (*Channa striatus*), the transcript sequence or genome information is lacking. To understand the molecular mechanisms on the pathogenicity of SHVV, the SSN-1 cell, originated from whole striped snakehead (*Channa striatus*) fry tissue, was used and the transcriptomic sequencing of SSN-1 cells upon SHVV infection was performed in this study.

A total of 3668 and 3536 DEGs were identified at 3 and 24 h poi. These DEGs were involved in many immune-related pathways,

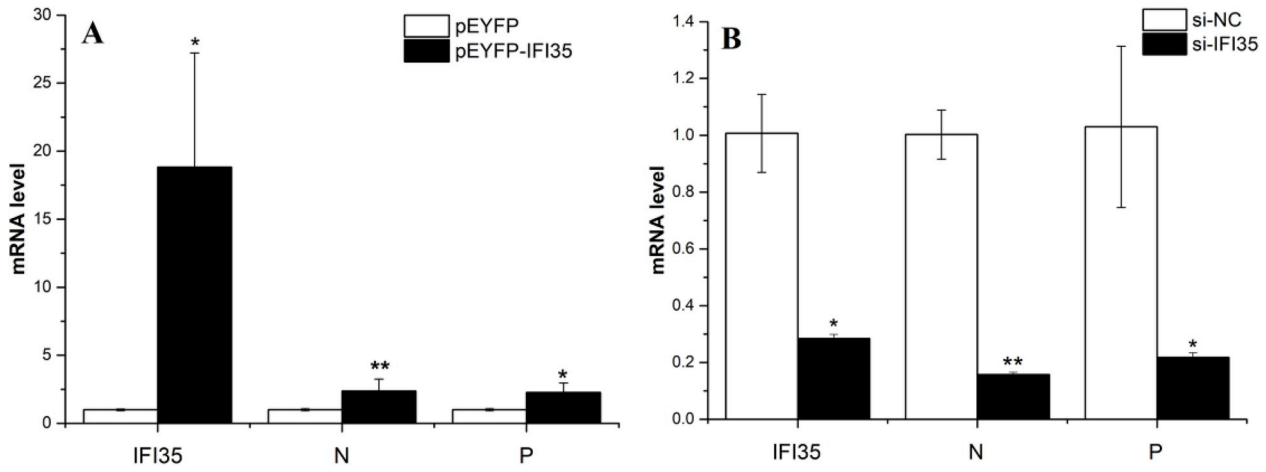

Fig. 7. IFI35 positively regulated SHVV replication. (A) Over expression of IFI35 in SSN-1 cells increases SHVV replication. The plasmid pEYFP-IFI35 or empty vector pEYFP were transfected into the SSN-1. At 24 h post-transfection, cells were collected to determine the expression level of IFI35 or infected with SHVV (MOI = 0.1) for 24 h to determine effects of IFI35 on SHVV replication. (B) Inhibition of IFI35 expression reduces SHVV replication. 100 nM IFI35 siRNA or control siRNA were transfected into the SSN-1. At 36 h post-transfection, cells were collected to determine the expression level of IFI35 or infected with SHVV (MOI = 0.1) for 24 h to determine effects of IFI35 on SHVV replication. Data presented in A and B are from three independent experiments, and values represent means and standard deviations (SD). * indicates $P < 0.05$; ** indicates $P < 0.01$.

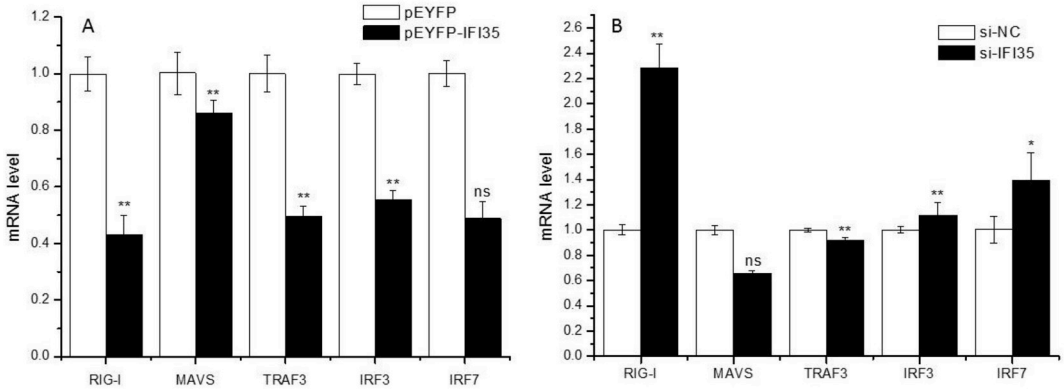

Fig. 8. IFI35 negatively regulated RIG-I pathway. (A) Over expression of IFI35 in SSN-1 cells decreases the mRNA level of genes in RIG-I pathway. The plasmid pEYFP-IFI35 or empty vector pEYFP were transfected into the SSN-1. At 24 h post-transfection, cells were infected with SHVV (MOI = 0.1) for 24 h to determine the expression level of RIG-I , MAVS , TRAF3 , IRF3 , IRF7. (B) Inhibition of IFI35 expression reduces the mRNA level of genes in RIG-I pathway. 100 nM IFI35 siRNA or control siRNA were transfected into the SSN-1. At 36 h post-transfection, cells were infected with SHVV (MOI = 0.1) for 24 h to determine effects of the expression level of RIG-I , MAVS , TRAF3 , IRF3 , IRF7. * indicates $P < 0.05$; ** indicates $P < 0.01$,ns indicates no significant difference.

including RIG-I like receptor signaling pathway, PI3K-Akt signaling pathway, MAPK signaling pathway, Toll-like receptor signaling pathway, and NF-kappa B signaling pathway. There is growing evidence that fish RIG-I can be activated and trigged the interferon response via a mitochondria associated signaling pathway [27–31]. Our results also showed that SHVV infection activated the RIG-I like receptor signaling pathway, leading to the production of IFN and several inflammatory cytokines (Fig. 5). Moreover, the expressions of the RIG-I, TRAF3, IRF7 and MAVS genes in SSN-1 cells upon SHVV infection were determined using qRT-PCR, and they were all significantly up regulated at 24 h post-infection, indicating that the SHVV infection activated the type I IFN pathway (Fig. 6).

The production of type I IFN results in hundreds of interferon-stimulated genes (ISGs). Most ISGs are known to exert antiviral effects to facilitate clearance of virus infection, such as IFI27, ISG20 and MX1 [32–35]. In addition, some ISGs have been reported to be negative regulators of the innate immune response and thus could support virus replication, such as ISG15, A20, RNF125, Ro52, ISG56 and Optineurin [32–37]. In this study, we found that SHVV replicated quite efficiently in SSN-1 cells, which drew our attention on whether some ISGs might positively regulated SHVV replication. One of the ISGs, IFI35, is a 35-kDa protein. It interacts with another ISG, N-myc interacting protein (Nmi), to form a 200–400 kDa high molecular mass complex (HMMC) in response to IFN-α treatment [38] and could be reduced in response to the treatment of cells with IFN-α/γ [39,40]. Recent report showed that IFI35 could target RIG-I for proteasome degradation in mammalian cells and facilitate vesicular stomatitis virus replication [41]. In our transcriptomic profiles, we also found that IFI35 was up regulated at 24 h poi in SSN-1 cells upon SHVV infection. The current role of IFI35 in fish cells was unknown. Therefore, the effects of IFI35 on SHVV replication were investigated. We found that IFI35 could function as a positive factor for SHVV replication (Fig. 7). To investigate if IFI35 regulated the antiviral signaling pathway, we examined the expression level of genes related to virus infection. The mRNA expression level of key genes in RIG-I like receptor signaling pathway changed, including RIG-I, MAVS, TRAF3, IRF3 and IRF7, all of which were known to be activated during VSV or SeV infection [42–44]. Overexpression of IFI35 could regulate the activity of RIG-I like receptor signaling pathway and the mRNA expression level of RIG-I , MAVS , TRAF3 , IRF3 were significantly downregulated, but (Fig. 8A). Conversely, the depletion of IFI35 gave rise to a reduction during SHVV infection, especially RIG-I, IRF3, IRF7 and TRAF3 (Fig. 8B). Whereas no significant alterations for

IRF7 and MAVS, and TRAF3 was significantly downregulated under both conditions. Since signal transduction was a complex system, we speculated that these genes may also be subject to feedback regulation by other signaling pathways. The results presented here indicated that IFI35 negatively regulated the host antiviral response mediated by RIG-I like receptor signaling pathway and we predicted IFI35 regulated host antiviral response mediated by RIG-I, IRF3 or TRAF3. However, the specific regulatory mechanism still needs further research. This is the first report about the effects of fish ISG IFI35 on SHVV replication. However, the effects of other fish ISGs on SHVV replication need further investigation.

Acknowledgments

This study was jointly supported by National Natural Science Fund (31572657, U31372563, 31872606); Special fund for marine economic development (GDME-2018C006) and Modern Fishery Development (GDMF-2018004) from the Administration of Ocean and Fisheries of Guangdong Province; and "Innovation and Strong Universities" special fund from the Department of Education of Guangdong Province (KA170500G). Jiangsu Agriculture Science and Technology Innovation Found (CX(18)2012), the Natural Science Foundation of the Jiangsu Higher Education Institutions of China (18KJB240003), the Natural Science Foundation of Jiangsu Province (BK20180915), the Projects of Shui Chan San Xin of Jiangsu Province (Y2016-33, D2017-3, D2015-15). V Sarath Babu was supported by Chinese Postdoctoral Science Foundation (189103).

Appendix A. Supplementary data

Supplementary data to this article can be found online at https://doi.org/10.1016/j.fsi.2018.11.031.

References

[1] David M. Knipe, Peter Howley, Rhabdoviridae, in: Douglas S. Lyles, Ivan V. Kuzmin, Charles E. Rupprecht (Eds.), Fields Virology, sixth ed., 2013, pp. 885–922 2013.
[2] P. de Kinkelin, B. Galimard, P. Bootsma, Isolation and identification of the causative agent of 'red disease' of pike (Esox lucius L.), Nature 241 (1973) 465–467.
[3] T. Kimura, M. Yoshimizu, S. Gorie, A new rhabdovirus isolated in Japan from cultured hirame (Japan flounder) paralichthys olivaceus and ayu plecoglossus altivelis, Dis. Aquat. Org. 1 (1986) 209–217.
[4] D.F. Amend, W.T. Yasutake, R.W. Mead, A haematopoietic virus disease of rainbow trout and sockeye salmon, Trans. Am. Fish. Soc. 98 (1969) 796–804.
[5] J. Kasornchandra, H.M. Engelking, C.N. Lannan, J.S. Rohovec, J.L. Fryer, Characteristics of three rhabdoviruses from snakerhead fish Ophicephalus striatus, Dis. Aquat. Org. 13 (1992) 89–94.
[6] H. Schutze, E. Mundt, T. Mettenleiter, C,Complete genomic sequence of viral hemorrhagic septicemia virus, a fish rhabdovirus, Virus Genes 19 (1999) 59–65.
[7] N. Fijan, Z. Petrinec, D. Sulimanovic, L.O. Zwillenberg, Isolation of the viral causative agent from the acute form of infectious dropsy of carp, Vet Arhiv Zagreb 41 (1971) 125–135.
[8] Q.Y. Zhang, Z.Q. Li, J.F. Gui, Isolation of a lethal rhabdovirus from the cultured Chinese sucker Myxocyprinus asiaticus, Dis. Aquat. Org. 42 (2000) 1–9.
[9] C. Du, Q. Zhang, C. Li, D. Miao, J. Gui, Induction of apoptosis in a carp leucocyte cell line infected with turbot (Scophthalmus maximus L.) rhabdovirus, Virus Res. 101 (2) (2004) 119–126.
[10] J.J. Tao, G.Z. Zhou, J.F. Gui, Q.Y. Zhang, Genomic sequence of Mandarin fish rhabdovirus with an unusual small non-transcriptional ORF, Virus Res. 132 (2008) 86–96.
[11] J.J. Tao, J.F. Gui, Q.Y. Zhang, Isolation and characterization of a rhabdovirus from co-infection of two viruses in Mandarin fish, Aquaculture 262 (2007) 1–9.
[12] T. Ou, R.L. Zhu, Z.Y. Chen, Q.Y. Zhang, Isolation and identification of a lethal rhabdovirus from farmed rice field eels Monopterus albus, Dis. Aquat. Org. 106 (2013) 197–206.
[13] W.W. Zeng, Q. Wang, Y.Y. Wang, C. Liu, H.R. Liang, X. Fang, S.Q. Wu, Genomic characterization and taxonomic position of a rhabdovirus from a hybrid snakehead, Arch. Virol. 159 (2014) 2469–2473.
[14] X. Liu, Y. Wen, X. Hu, W. Wang, X. Liang, J. Li, V. Vakharia, L. Lin, Breaking the host range:Mandarin fish is susceptible to a vesiculovirus derived from snakehead fish, J. Gen. Virol. 96 (2015) 775–781.
[15] M.I. Thurston, D.W. Pallett, M. Cortina-Borja, et al., The incidence of viruses in wild Brassica nigra in Dorset (UK), Ann. Appl. Biol. 139 (2001) 277–284.
[16] S. Reed, b Shabmana, et al., Deep sequencing identifies noncanonical editing of ebola and marburg virus RNAs in infected cells, American society for microbiology 5 (2014) 1–11.
[17] A. Acevedo, L. Brodsky, R. Andino, Mutational and fitness landscapes of an RNA virus revealed through population sequencing, Nature 505 (2014) 686–690.
[18] Peter J.A. Cock, Christopher J. Fields, Naohisa Goto, Michael L. Heuer, Peter M. Rice, The Sanger FASTQ file format for sequences with quality scores, and the Solexa/Illumina FASTQ variants, Nucleic Acids Res. 38 (6) (2010) 1767–1771.
[19] S.F. Altschul, W. Gish, W. Miller, E.W. Myers, D.J. Lipman, Basic local alignment search tool, J. Mol. Biol. 215 (3) (1990) 403–410.
[20] A. Conesa, S. Gotz, J.M. Garcia-Gomez, J. Terol, M. Talon, M. Robles, Blast2GO: A universal tool for annotation, visualization and analysis in functional genomics research, Bioinformatics 21 (2005) 3674–3676.
[21] T.D. Schmittgen, K.J. Livak, Analyzing real-time PCR data by the comparative C-T method, Nat. Protoc. 3 (6) (2008) 1101–1108.
[22] G. Grabherr Manfred, et al., Trinity: reconstructing a full-length transcriptome without a genome from RNA-Seq data, Nat. Biotechnol. 29 (7) (2011) 644–652.
[23] G. Pertea, X. Huang, F. Liang, V. Antonescu, R. Sultana, S. Karamycheva, Y. Lee, J. White, F. Cheung, B. Parvizi, J. Tsai, J. Quackenbush, TIGR Gene Indices clustering tools (TGICL): a software system for fast clustering of large EST datasets, Bioinformatics 19 (5) (2003) 651–652.
[24] M.H. Shi, R. Huang, F.K. Du, Y.P. Wang, RNA-seq profiles from grass carp tissues after reovirus (GCRV) infection based on singular and modular enrichment analyses, BMC Genomics 16 (1) (2015) 184.
[25] R. Wang, L. Sun, L. Bao, J. Zhang, Y. Jiang, J. Yao, L. Song, J. Feng, S. Liu, Z. Liu, Bulk segregant RNA-seq reveals expression and positional candidate genes and allele-specific expression for disease resistance against enteric septicemia of catfish, BMC Genomics 14 (2013) 929.
[26] Y. Mu, F. Ding, P. Cui, Transcriptome and expression profiling analysis revealed changes of multiple signaling pathways involved in immunity in the large yellow croaker during Aeromonas hydrophila infection, BMC Genomics 9 (22) (2010) 506.
[27] V. Hornung, J. Ellegast, S. Kim, K. Brzózka, A. Jung, H. Kato, H. Poeck, S. Akira, K.K. Conzelmann, M. Schlee, 5'-Triphosphate RNA is the ligand for RIG-I, Science 314 (2006) 994–997.
[28] A. Pichlmair, O. Schulz, C.P. Tan, T.I. Naslund, P. Liljestrom, F. Weber, C. Reis e Sousa, RIG-I-mediated antiviral responses to single-stranded RNA bearing 5'-phosphates, Science 314 (2006) 997–1001.
[29] W. Chen, Y. Hu, P. Zou, S. Ren, P. Nie, M. Chang, MAVS splicing variants contribute to the induction of interferon and interferon-stimulated genes mediated by RIG-I-like receptors, Dev. Comp. Immunol. 49 (2015) 19–30.
[30] J. Zhou, M. Chang, P. Nie, J. Chris, Origin and evolution of the RIG-I like RNA helicase gene family, BMC Evol. Biol. 9 (2009).
[31] P. Zou, M. Chang, Y. Li, S. Huan Zhang, J. Fu, S. Chen, P. Nie, Higher antiviral response of RIG-I through enhancing RIG-I/MAVS-mediated signaling by its long insertion variant in zebrafish, Fish Shellfish Immunol. 43 (2014) 13–24.
[32] Y. Itsui, N. Sakamoto, M. Kurosaki, N. Kanazawa, Y. Tanabe, T. Koyama, Y. Takeda, M. Nakagawa, S. Kakinuma, Y. Sekine, S. Maekawa, N. Enomoto, M. Watanabe, Expressional screening of interferon-stimulated genes for antiviral activity against hepatitis C virus replication, J. Viral Hepat. 13 (2006) 690–700.
[33] D. Jiang, H. Guo, C. Xu, J. Chang, B. Gu, L. Wang, T.M. Block, J.T. Guo, Identification of three interferon-inducible cellular enzymes that inhibit the replication of hepatitis C virus, J. Virol. 82 (2008) 1665–1678.
[34] M.J. Kim, S.Y. Hwang, T. Imaizumi, J.Y. Yoo, Negative feedback regulation of RIG-I-mediated antiviral signaling by interferon-induced ISG15 conjugation, J. Virol. 82 (2008) 1474–1483.
[35] I.E. Wertz, K.M. O Rourke, H. Zhou, M. Eby, L. Aravind, S. Seshagiri, P. Wu, C. Wiesmann, R. Baker, D.L. Boone, A. Ma, E.V. Koonin, V.M. Dixit, De-ubiquitination and ubiquitin ligase domains of A20 downregulate NF-kappaB signaling, Nature 430 (2004) 694–699.
[36] K. Arimoto, H. Takahashi, T. Hishiki, H. Konishi, T. Fujita, K. Shimotohno, Negative regulation of the RIG-I signaling by the ubiquitin ligase RNF125, Proc. Natl. Acad 104 (2007) 7500–7505.
[37] R. Higgs, J. Ni Gabhann, N. Ben Larbi, E.P. Breen, K.A. Fitzgerald, C.A. Jefferies, The E3 ubiquitin ligase Ro52 negatively regulates IFN-beta production post-pathogen recognition by polyubiquitin-mediated degradation of IRF3, J. Immunol. 181 (2008) 1780–1786.
[38] Y. Li, C. Li, P. Xue, B. Zhong, A.P. Mao, Y. Ran, H. Chen, Y.Y. Wang, F. Yang, H.B. Shu, ISG56 is a negative-feedback regulator of virus-triggered signaling and cellular antiviral response, Proc. Natl. Acad 106 (2009) 7945–7950.
[39] J. Mankouri, R. Fragkoudis, K.H. Richards, L.F. Wetherill, M. Harris, A. Kohl, R.M. Elliott, A. Macdonald, Optineurin negatively regulates the induction of IFNbeta in response to RNA virus infection, PLoS Pathog. 6 (2010) e1000778.
[40] X. Zhou, J. Liao, A. Meyerdierks, L. Feng, L. Naumovski, E.C. Bottger, M.B. Omary, Interferon-alpha induces nmi-IFP35 heterodimeric complex formation that is affected by the phosphorylation of IFP35, J. Biol. Chem. 275 (2000) 21364–21371.
[41] F.C. Bange, U. Vogel, T. Flohr, M. Kiekenbeck, B. Denecke, E.C. Bottger, IFP 35 is an interferon-induced leucine zipper protein that undergoes interferon-regulated cellular redistribution, J. Biol. Chem. 269 (1994) 1091–1098.
[42] X. Wang, L.M. Johansen, H.J. Tae, E.J. Taparowsky, IFP 35 forms complexes with B-ATF, a member of the AP1 family of transcription factors, Biochem. Biophys. Res. Commun. 229 (1996) 316–322.
[43] P.X. Das, D. Dinh, A.K. Panda, Pattnaik Interferon-inducible protein IFI35 negatively regulates RIG-I antiviral signaling and supports vesicular stomatitis virus replication, J. Virol. 88 (2014) 3103–3113.
[44] R.E. Randall, S. Goodbourn, Interferons and viruses: an interplaybetween induction, signaling, antiviral responses and virus counter measures, J. Gen. Virol. 89 (2008) 1–47.